THE JOURNAL OF PHYSICAL CHEMISTRY C

Article

pubs.acs.org/JPCC

Dissociative Adsorption of Hydrogen on PdO(101) Studied by HRCLS and DFT

N. M. Martin,[†] M. Van den Bossche,[‡] H. Grönbeck,[‡] C. Hakanoglu,[§] J. Gustafson,[†] S. Blomberg,[†] M. A. Arman,[†] A. Antony,[§] R. Rai,[§] A. Asthagiri,[∥] J. F. Weaver,[§] and E. Lundgren*[,†]

[†]Division of Synchrotron Radiation Research, Lund University, Lund, Sweden

[‡]Competence Centre for Catalysis and Department of Applied Physics, Chalmers University of Technology, Göteborg, Sweden

[§]Department of Chemical Engineering, University of Florida, Gainesville, Florida, United States

[∥]William G. Lowrie Department of Biomolecular and Chemical Engineering, The Ohio State University, Columbus, Ohio, United States

ABSTRACT: High-resolution core-level spectroscopy (HRCLS) and density functional theory (DFT) calculations have been used to investigate the adsorption and dissociation of hydrogen on a PdO(101) film grown on Pd(111). Energy-dependent measurements of the O 1s and Pd $3d_{5/2}$ binding energies enable identification of surface components that correspond to undercoordinated Pd and O atoms. HRCLS data obtained at 110 K, after hydrogen exposure at the same temperature, reveal hydrogen adsorption and formation of Pd-H and O-H groups. Adsorption at room temperature results instead in complete reduction of the oxide. The experimental results are supported by the DFT calculations of core-level shifts and barriers for water formation.

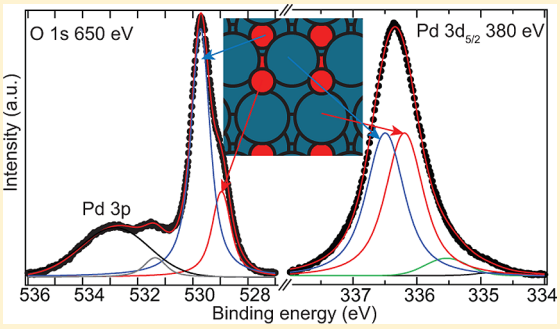

I. INTRODUCTION

Supported palladium particles are commonly used for the catalytic oxidation of CO, methane, and hydrocarbons in, for example, automotive emission control. Whereas the detailed nature of the active site in CO oxidation over Pd has been extensively investigated during the past few years,[1−4] less attention has been paid to the character of the active site in methane and hydrocarbon oxidation. Although early reports suggested that an increased activity of Pd catalysts could be attributed to the formation of a bulk like PdO phase,[5−7] it is only recently that the importance of special facets with undercoordinated Pd atoms has been highlighted.[8−10] Hydrogen oxidation is a key step in the catalytic oxidation of hydrocarbons and other organic molecules and motivates fundamental studies of how hydrogen interacts and reacts on PdO surfaces.

Another transition metal that has been studied extensively during the past few years is ruthenium, motivated mainly by numerous applications in catalysis.[9−11] In particular, it has been reported that the increased activity for CO oxidation over Ru at high oxygen partial pressures can be traced to the formation of $RuO_2(110)$, which provides active adsorption sites, namely, undercoordinated Ru atoms at the surface of this oxide.[12,13] Moreover, the interaction of hydrogen with the $RuO_2(110)$ surface has been studied with a combination of experimental and theoretical methods.[14] It has been observed that hydrogen adsorbs molecularly at the undercoordinated Ru atoms. The molecule dissociates at temperatures below 120 K, whereby O-H groups are formed. As both $RuO_2(110)$ and PdO(101) expose undercoordinated metal atoms to the gas phase, some similarities can be expected as to the adsorption and reaction of simple molecules.

The interaction of oxygen with Pd has been intensively studied in the literature.[3,9,15−22] In particular, the oxidation of Pd(111) with molecular oxygen shows that the oxygen atoms initially arrange in a $p(2 \times 2)$ structure (0.25 ML), whereas a two-dimensional (2D) oxide ($\sqrt{6} \times \sqrt{6}$, 0.67 ML) is formed at higher coverages, the so-called "root6" structure[20] with a Pd_5O_4 stoichiometry (1 ML equals the surface atom density of Pd(111)). This surface oxide has two types of Pd atoms that are either 2- or 4-fold coordinated to O atoms and two types of O atoms that are either 3- or 4-fold coordinated to Pd atoms. Bulk oxidation has been found to proceed through PdO seeds growing on the 2D oxide.[22,23] With increasing oxygen coverage, the PdO seeds grow in size and transform to more stable particles that agglomerate into a PdO film. PdO crystallizes in a tetragonal structure where all Pd atoms have an equivalent planar coordination to four O atoms and all O atoms are tetrahedrally surrounded by four Pd atoms. Kan and Weaver have demonstrated that a well-ordered PdO(101) film can be grown in ultra-high-vacuum conditions (UHV) by oxidizing a Pd(111) surface with an atomic oxygen beam.[21,22] PdO(101) is

Received: April 14, 2013
Revised: May 31, 2013
Published: June 4, 2013

   dx.doi.org/10.1021/jp4036698 | J. Phys. Chem. C 2013, 117, 13510−13519

an interesting model surface as it contains undercoordinated metal and O atoms. The film grown at 500 K was reported to have a thickness of about 12 Å (4−5 PdO layers) and an oxygen coverage of 3−4 ML. Furthermore, experiments under conditions close to real application conditions have shown that PdO(101) forms preferentially also upon oxidation of Pd(100).[3,8,24]

Hydrogen adsorption on PdO(101) has been previously investigated both experimentally and theoretically. A DFT-based study by Blanco-Rey et al.[25] suggests that hydrogen adsorbs on the undercoordinated (3-fold coordinated) Pd atoms and that water formation is associated with high activation energies. Soon after, Hakanoglu et al.[27] used temperature-programmed desorption (TPD) combined with DFT calculations to study the adsorption of hydrogen on PdO(101). It was concluded that hydrogen dissociatively adsorbs below 100 K via a molecularly adsorbed precursor state and that most of the dissociated hydrogen reacts with the surface to produce water desorbing at about 350 K. Evidence was presented that the undercoordinated Pd sites are needed to activate and dissociate hydrogen on PdO(101). From the DFT calculations, it was predicted that molecularly adsorbed hydrogen can react with the surface oxygen atoms to form O-H groups (H_2-Pd_{3f} + O_{3f} → H-Pd_{3f} + H-O_{3f}). Here, Pd_{3f} and O_{3f} denote 3-fold coordinated Pd and O atoms, respectively.

In this study, we have characterized the interaction of hydrogen with a PdO(101) thin film in UHV conditions by the use of high resolution core-level spectroscopy (HRCLS) and DFT calculations. The HRCLS measurements provide resolution to discriminate between surface atoms with different coordination. The adsorption of hydrogen on the PdO(101) surface was studied in UHV at both 110 and 300 K. Changes in the O 1s and Pd 3d spectra observed upon dosing 10 L of hydrogen reveal that hydrogen adsorbs dissociatively on PdO(101) at 110 K. The calculated core-level shifts (CLSs) for the dissociation of hydrogen on PdO(101) and formation of Pd-H and O-H groups support this interpretation. Dosing 1 × 10^{-8} mbar hydrogen at 300 K on the PdO(101) results in extensive reduction of the oxide. The DFT calculations suggest a possible mechanism together with activation energies for the formation and desorption of water. The presented results agree well with previous reports of hydrogen adsorption on PdO(101).[25,27]

II. EXPERIMENTAL METHODS

The measurements were performed at beamline I311 at the MAX IV Laboratory in Lund, Sweden.[28] The sample, a Pd(111) single crystal, was mounted on a tungsten wire through which it could be heated to high temperatures by applying an electric current and the temperature was measured by a chromel−alumel thermocouple spot-welded on the back side of the crystal. After repeated cycles of sputtering with Ar^+ ions and annealing up to 1050 K, the surface cleanliness was checked by low-energy electron diffraction (LEED) and X-ray photoelectron spectroscopy (XPS). For the oxidation process, we used atomic oxygen produced by a thermal gas cracker from Dr. Eberl MBE Komponenten GMBH with a flux of the oxygen atoms of about 10^{15} atoms/s and a cracking efficiency of about 15% during our measurements. The background pressure was 5 × 10^{-7} mbar, and the sample was held at 500 K during the atomic oxygen exposures. The oxidation was performed following the preparation methods described previously to produce a high-quality PdO(101) film, and the LEED pattern was found to resemble the pattern from the PdO(101) reported earlier.[21]

The XPS measurements were recorded using normal emission and photon energies of 380 eV for the Pd $3d_{5/2}$ and 650 eV for the O 1s line, respectively. For the analysis of the recorded photoelectron spectroscopy spectra, a deconvolution procedure involving a Doniach Šunjić line shape convoluted with a Gaussian was used. The binding energies were calibrated to the Fermi edge, and a polynomial background was subtracted. All spectra are normalized to the main peak for the energy-dependent measurements, or to the background for the other measurements.

III. COMPUTATIONAL METHOD

The density functional theory (DFT) was applied with the gradient-corrected exchange-correlation functional according to Perdew, Burke, and Ernzerhof (PBE).[29] In particular, the VASP code was used.[30−32] The one-electron Kohn−Sham orbitals were expanded in a plane-wave basis set with a kinetic energy cutoff of 450 eV. To describe the interaction between the valence electrons and the core, PAW potentials[33,34] were used for all elements (palladium, oxygen, and hydrogen). A p(2 × 1) surface cell was considered for PdO(101). The surface was modeled as a slab with four or seven PdO trilayers in the calculations of the energy landscape and core-level shifts, respectively. The slabs were separated by at least 12 Å in the direction normal to the surface. The use of four trilayers in the calculations of the energetics is motivated by the computational cost in evaluation of the reaction barriers. Adsorption energies were calculated also with a seven trilayer slab and were found to be consistently lowered by 0.1 eV. A seven trilayer slab is needed in the calculations of the core-level shifts to ensure a proper bulk reference. Reciprocal space integration over the Brillouin zone was approximated with finite sampling using a 4 × 4 × 1 Monkhorst−Pack grid.[35,36] Geometry optimizations were carried out without any constraints, and the structures were considered relaxed when the largest force in the system was smaller than 0.01 eV/Å. Nudged elastic band calculations[37] were performed to obtain activation energies. Zero-point energy corrections to adsorption energies and transition-state barriers were calculated by vibrational analysis using finite differences.

The surface core-level shifts (CLS) were evaluated by use of pseudopotentials that were generated with an electron hole in either the 3d shell (Pd) or the 1s shell (O).[38] The CLS were calculated with respect to a bulk reference, represented by an atom in the center of the slab (the mid trilayer). To maintain charge neutrality, a homogeneous jellium background was included. This approach was preferred over the alternative method where an extra valence electron is added. The latter method is problematic for nonmetallic systems with a low density of states near the Fermi energy. Experiments suggest that PdO is a semiconductor with a small direct band gap of 0.7−1 eV.[39] Although the applied functional describes PdO as a metal, the density of states near the Fermi energy is small.

IV. RESULTS AND DISCUSSION

A. Oxidation of Pd(111). The PdO(101) surface has been previously characterized experimentally with TPD,[22] (LEED),[21,22] and scanning tunneling microscopy (STM)[40] and theoretically by DFT.[41,42] In summary, the PdO(101) film grown on Pd(111) at 500 K has been reported to have a

dx.doi.org/10.1021/jp4036698 | J. Phys. Chem. C 2013, 117, 13510−13519

coverage of 3−4 ML and to consist of alternating rows of Pd and O atoms, which, at the surface, will have different coordinations as compared to the bulk (3- or 4-fold coordinated, whereas all atoms are 4-fold coordinated in the bulk). The structure of the PdO(101) surface is shown in Figure 1. The coverage of each type of undercoordinated atom

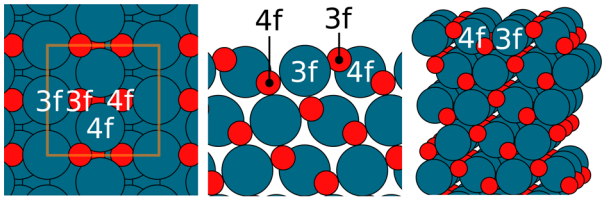

Figure 1. Top, side, and tilted views of the PdO(101) surface. The 3- and 4-fold coordinated O and Pd atoms are indicated. The (1 × 2) surface unit cell is shown in orange. Atomic color codes: blue, Pd; red, O.

is 0.35 ML in terms of Pd atoms in the Pd(111) surface. Each layer contains 0.7 ML of Pd atoms and 0.7 ML of O atoms. The film has been described in detail in the literature, and we refer the reader to refs 10, 21, and 40 for further details.

In Figure 2a, we show the O 1s and Pd $3d_{5/2}$ core-level spectra recorded at normal emission from PdO(101) grown on Pd(111). The spectra were recorded after oxidation of the Pd(111) surface with atomic oxygen at 500 K and an oxygen base pressure of 5×10^{-7} mbar. The main peak in the Pd $3d_{5/2}$ spectrum originates from oxidized Pd atoms in the PdO film and can be deconvoluted with two components (blue and red). The minor components are attributed to metallic Pd bulk (black) and a thin surface oxide (green), from a 2D "root6" structure as it was previously described. The O 1s spectrum recorded with a photon energy of 650 eV has an intense oxide peak in addition to the Pd 3p peak that appears at about 533 eV. The oxide peak has a shoulder on the low binding energy side and can be decomposed into two components (blue and red) with a ratio of 0.4. The weak component at about 531.5 eV (gray) is ascribed to OH, as will be described in more detail in the next section.

An unambiguous assignment of surface and bulk components is enabled by variation of the incident X-ray photon energy. The energy dependence of the Pd $3d_{5/2}$ features is depicted in Figure 2c,e. When the photon energy is increased, the component with low binding energy (red) decreases as compared to the component with high binding energy (blue). Moreover, the intensity of the metallic Pd bulk peak is increasing. Thus, it can be concluded that the low binding energy component (red) originates from Pd atoms in the surface. On the other hand, the peak at higher binding energies (blue) contains contributions from both surface and bulk atoms. At a low photon energy (380 eV), the escaping electrons arise from the near surface region (their mean free path is short at these energies) and the intensity ratio between the two components is 1. At higher energies, the bulk atoms are probed and the intensity is increased as compared to the feature at lower binding energies. The low energy feature (red) is assigned to Pd atoms coordinated to three oxygen atoms, whereas the high energy feature (blue) is connected to Pd atoms coordinated to four oxygen atoms. 4-Fold coordinated atoms are present both on the surface and in the bulk; the surface structure is shown as an inset in Figure 2. In similarity with the Pd results, the energy-dependent measurements of the O 1s spectra (Figure 2b,d) show a decrease of the low binding

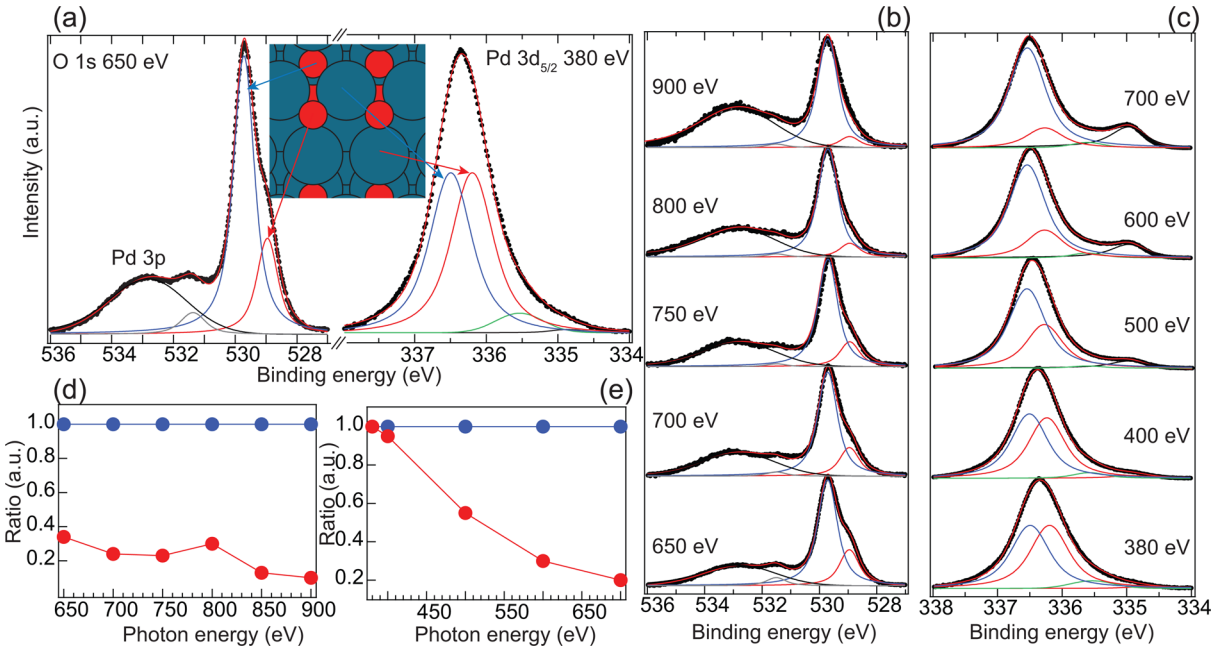

Figure 2. High-resolution core-level spectra obtained from the PdO(101) film grown on Pd(111). (a) The O 1s is recorded with a photon energy of 650 eV and the Pd $3d_{5/2}$ with 380 eV. The Pd $3d_{5/2}$ spectrum can be decomposed into four components. The components can be identified as Pd in the bulk (black), Pd from a surface oxide (green), and Pd atoms from the PdO (3-fold coordinated, red; 4-fold coordinated, blue). The O 1s peak exhibits a shoulder on the low binding energy side. The inset shows a top view of the PdO(101) surface. Energy-dependent measurements from (b) O 1s level and (c) Pd $3d_{5/2}$ level. The integrated area from (d) O 1s and (e) Pd $3d_{5/2}$ components. Using energy-dependent core-level measurements, we are able to assign the different experimental O 1s and Pd 3d core-level shifts unambiguously to surface and bulk components, respectively (see text for details).

dx.doi.org/10.1021/jp4036698 | J. Phys. Chem. C 2013, 117, 13510−13519

energy component (red) upon increased photon energy. This component is consequently assigned to surface O atoms that are 3-fold coordinated to Pd atoms. The high binding energy component (blue) is assigned to 4-fold coordinated O atoms that are present both on the surface and in the bulk. For the lowest photon energies employed (650 eV for O 1s and 380 eV for Pd3d), the O 1s spectrum is more bulk-sensitive than the Pd 3d spectrum, and consequently, the bulk and surface components are more intense than the sole surface component in the O 1s spectrum. Similar XPS signatures have previously been observed upon oxidation of the Pd(100) surface at 270 °C and 0.5 mbar O_2,[24] which indicates that a similar PdO film is grown on Pd(100) and Pd(111) upon oxidation.

B. Hydrogen Adsorption on PdO(101) at 110 K. After the PdO(101) reference system was established, the chemistry of hydrogen adsorption could be investigated. In Figure 3a,b,

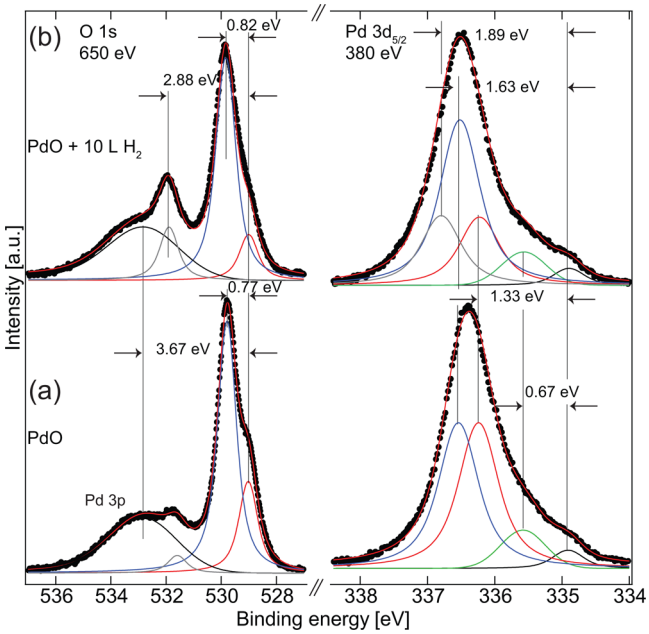

Figure 3. (a) HRCLS signature of the PdO(101) film grown on Pd(111). In the Pd $3d_{5/2}$ spectra, a contribution from a surface oxide (green) and Pd bulk component (black) may still be observed. The shifts are given with respect to the bulk Pd (Pd $3d_{5/2}$) or the O_{3f} atoms (O 1s). (b) Pd $3d_{5/2}$ and O 1s HRCL spectra after dosing 10 L of H_2 on the PdO(101) surface at 110 K. As hydrogen is adsorbing on the PdO(101), the component assigned to surface O atoms in the O 1s (red) decreases and a new component appears at about 2.9 eV toward higher binding energy (gray). In the Pd $3d_{5/2}$ level, the component from the undercoordinated Pd atoms (red) also decreases upon H_2 exposure, and a new component appears at higher binding energy (gray).

the Pd $3d_{5/2}$ and O 1s spectra are presented before and after exposure to 10 L of hydrogen at 110 K. The shifts of the different components are given with respect to the metal bulk Pd and 3-fold coordinated surface O atoms, respectively. Upon hydrogen exposure, the intensity of the Pd_{3f} component at the surface of the oxide decreases (red component) and a new component at 0.55 eV higher binding energy is observed (gray); see the right panel of Figure 3b. In the O 1s spectrum (Figure 3b, left panel), the intensity of the shoulder on the low binding energy side (O_{3f}) decreases and a new component appears at about 2.9 eV higher binding energy (gray). The measurements show that both the Pd_{3f} and the O_{3f} atoms at the surface of the PdO(101) film are affected by the hydrogen adsorption, which strongly suggests that hydrogen dissociates at the PdO(101) surface.

The experiments were repeated using the same conditions, but dosing higher amounts of hydrogen. However, no major changes were observed in the Pd 3d and O 1s spectra as compared to the results shown in Figure 3. Thus, 10 L of hydrogen is sufficient to obtain a saturation coverage in this study. Given that our assignments of the core-level components are correct (see below for the theoretical support) and assuming a perfect PdO(101) surface layer, it is possible to estimate the number of Pd_{3f} and O_{3f} atoms that are directly affected by the hydrogen atoms by monitoring the decrease of the intensity of the O_{3f} and Pd_{3f} components. In this way, we observe a 50% intensity decrease of the component from O_{3f} atoms and a 50% decrease of the component from Pd_{3f} atoms. It can, therefore, be concluded that 50% of the Pd_{3f} and 50% of the O_{3f} atoms are covered with H atoms, with an uncertainty of ±10%.

The saturation coverage found in the present study is lower than the saturation coverage found previously from TPD measurements.[27] However, in ref 27, the hydrogen adsorption was done at lower temperature, 75 K, which may affect the total hydrogen coverage. For instance, on the basis of the H_2O yields obtained after H_2 adsorption, a decreasing hydrogen coverage was found with increasing adsorption temperature, in agreement with the present observation. Furthermore, in the present study, as in ref 27, the PdO(101) film has imperfections that cause additional uncertainties with respect to the coverage estimation. In a very recent study by Kasper et al.,[43] oxidation of Pd(111) by molecular O_2 was investigated by surface X-ray diffraction (SXRD) measurements and it was observed that PdO(100) may coexist with PdO(101). Thus, we do not exclude the possibility that another surface orientation may be present on the PdO surface influencing the hydrogen adsorption process. We also cannot exclude the possibility that some oxygen vacancies were created during PdO(101) film preparation due to reactions between the surface and the residual gas. It should also be noted that the coverage calibration performed in the TPD measurements[27] also introduces some uncertainties.

To facilitate the interpretation of the XPS measurements, a set of DFT calculations was performed for hydrogen adsorption onto PdO(101). The potential energy landscape was investigated, and core-level shifts (CLSs) were evaluated for stable structures. Although the measurements were performed on a film of PdO(101) supported on Pd(111), the calculations were done on a PdO(101) slab. This is justified by the fact that the chemical and electronic properties of the PdO(101) film are converged to the PdO bulk values.[24,42]

The potential energy landscape is shown in Figure 4, where zero energy corresponds to a clean PdO(101) surface and H_2 in the gas phase. Hydrogen is molecularly adsorbed with an adsorption energy of −0.33 eV. The stable configuration corresponds to the H_2 molecular axis aligned along the row with Pd_{3f} atoms. The H−H bond in adsorbed H_2 (0.84 Å) is clearly elongated as compared to the gas-phase molecule (0.75 Å). The Pd_{3f}−H_2 distance is 1.70 Å. Hydrogen adsorption on PdO(101) has previously been considered computationally in refs 25 and 27 using similar methods as the present one. In ref 25, H_2 was predicted to be adsorbed perpendicularly to the Pd_{3f} atoms. However, this configuration is here found to be higher in energy by ∼0.1 eV, in agreement with DFT results reported

dx.doi.org/10.1021/jp4036698 | J. Phys. Chem. C 2013, 117, 13510−13519

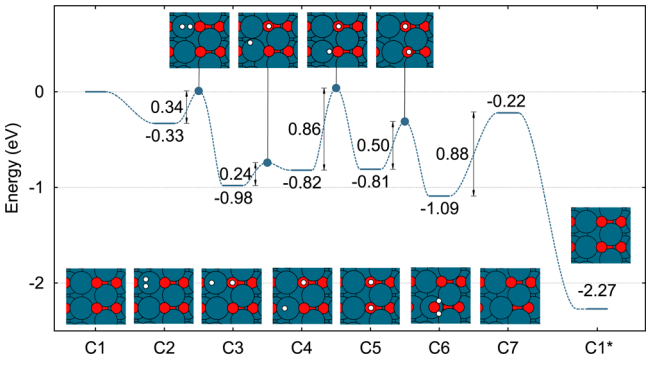

Figure 4. Potential energy profile for water formation on PdO(101). The zero-energy reference corresponds to the clean PdO(101) slab and the H_2 molecule in the gas phase. The structural models at the bottom show stable structures, whereas the transition-state structures are shown at the top. Atomic color codes: blue, Pd; red, O; and white, H (see text for details).

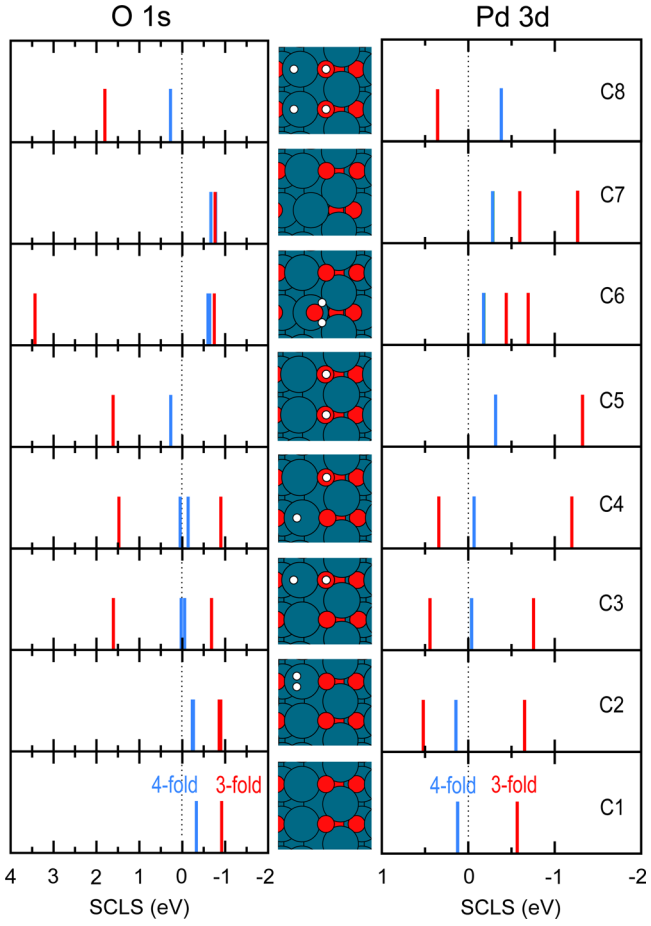

Figure 5. Middle column: Top views of the optimized structures with hydrogen present on the PdO(101) surface in various configurations with 0.5 ML (C1−C7) and 1 ML (C8) hydrogen coverage. Atomic color codes: blue, Pd; red, O; white, H. Left and right columns report O 1s and Pd 3d CLS, respectively. The results for the 3- and 4-fold coordinated surface atoms are indicated by the red and blue lines, following the color code in Figures 2 and 3. Thicker lines represent a larger number of atoms with the same binding energy.

by Hakanoglu et al.[27] Dissociation of H_2 proceeds by the rotation and subsequent scission of the molecular bond. The barrier for this process is calculated to be 0.34 eV. The formation of an O_{3f}-H group and a Pd_{3f}-H group is energetically preferred, and the adsorption energy is −0.98 eV. The Pd_{3f}–H and O_{3f}–H bond lengths are 1.55 and 0.98 Å, respectively. The hopping of a H atom along the Pd_{3f} row is associated with a barrier of 0.24 eV. Diffusion of a hydrogen atom from a Pd_{3f} to an O_{3f} site has a high barrier of 0.86 eV. Note that the three configurations with adsorbed hydrogen atoms (C3, C4, and C5) are fairly close in energy. Water can be formed via a Mars van Krevelen process from C5 wherein neighboring O_{3f}-H groups disproportionate and the resulting water molecule moves to a Pd_{3f} site. The reaction is exothermic within the current computational scheme with a barrier of 0.50 eV. The desorption energy for H_2O is 0.89 eV. In C6, water is adsorbed with a bond angle of 105.3° and a H−O distance of 0.98 Å. These values are close to the gas-phase values of 104.5° and 0.97 Å, respectively. Water formation from adsorbed hydrogen was considered in ref 25 with a mechanism where the Pd_{3f}-H and O_{3f}-H groups in C3 react. However, the barrier for that path is considerably larger (1.94 eV) than the barriers determined for the pathway shown in Figure 4. The potential energy landscape reveals that H_2 dissociation and hydrogen diffusion along the Pd_{3f} rows should be possible at low temperatures. Water formation at low temperature is, on the other hand, hindered by high barriers for hydrogen diffusion (C4 to C5). We note that the barrier for H-hopping directly between the two O_{3f} sites has a high barrier of 1.5 eV. In configuration C1*, the oxygen vacancy created upon H_2O formation has been healed by half an oxygen molecule. The energy corresponds to the enthalpy of formation for H_2O. The calculated value (−2.27 eV) is close to the experimental value (−2.51 eV).[26]

The CLS (Pd 3d and O 1s) for the stable structures are reported in Figure 5. The shifts are calculated for all atoms in the topmost trilayer with respect to (4-fold coordinated) atoms in the center of the slab. For the clean surface (C1), a large negative shift is calculated for Pd_{3f} (−0.57 eV), whereas a small positive shift (0.12 eV) is predicted for Pd_{4f}. This is in fair agreement with the experiments, although a smaller splitting (0.3 eV) between the surface components is measured. This difference between the calculated CLS and the experimentally observed shift has been observed previously[24] and may be due to the applied approximation to the exchange-correlation functional, which does not describe the band gap of PdO correctly. Adsorption of either molecular or atomic hydrogen on Pd_{3f} atoms induces marked shifts in the binding energies; see configurations C2, C3, and C4. Adsorption causes the CLS to be positive by ∼0.4 eV. Interestingly, the formation of OH groups has pronounced effects on the neighboring Pd_{3f} CLS. The shifts in C4 and C5 are −1.3 eV. Formation of water (C6) makes the average shift similar to the clean surface. Desorption of water produces a Pd_{3f} shift, which again is about −1.3 eV. The Pd_{4f} component is changing from being slightly positive to slightly negative during the process of water formation.

The O 1s shifts are both negative for the clean surface, with the largest shift predicted for O_{3f} atoms. Molecular H_2 adsorption affects the O 1s CLS in a minor fashion, whereas the formation of OH or H_2O has pronounced effects. The O 1s levels for OH (C3, C4, C5) and H_2O (C6) have shifts of 1.6 and 3.4 eV, respectively. The large shifts are consistent with the experiments as well as previous calculations of OH groups on MgO(100).[44] During the reaction, small variations are predicted in the shifts of the O_{4f} component.

dx.doi.org/10.1021/jp4036698 | J. Phys. Chem. C 2013, 117, 13510−13519

For comparison, also the case of doubled coverage was considered, namely, one H atom on every 3-fold surface atom (C8). The higher coverage has only minor effects on the CLS. The positive Pd 3d shifts for Pd_{3f} are slightly smaller, and the positive O 1s shifts for O_{3f} are slightly larger. Note that a completely hydrogen-covered PdO(101) surface would make the Pd_{3f} and O_{3f} signatures disappear. This is not observed in the measured spectra (Figure 3). The adsorption energy per hydrogen molecule is −1.06 eV in this case, which should be compared to the value in Figure 4 for half coverage (C3), which is −1.41 eV. Thus, the average binding energy is decreasing by increasing the hydrogen coverage.

By comparing the calculated CLS in Figure 5 with the experimentally determined shifts as illustrated in Figure 3, we find that the half coverage structures (C3 and C4) fit very well with the measurements. A clear comparison is shown in Figure 6a,b, where the calculated CLS for the C3 (a) and C4 (b) structures are indicated as lines at the bottom of each spectrum. There is a good agreement between the calculated CLS of OH groups as well as for Pd_{3f} atoms with adsorbed atomic hydrogen. Thus, the emerging picture is that H_2 initially adsorbs in molecular form on the Pd_{3f} atoms of PdO(101) but dissociates at 110 K to give rise to O_{3f}-H and Pd_{3f}-H groups, as illustrated by the C3 and C4 models. No evidence for water formation was observed in the HRCL spectra upon H_2 adsorption on PdO(101) at 110 K. Adsorbed H_2O should give rise to clear signatures in the O 1s spectra. The absence of water at this temperature is consistent with the calculated high barriers associated with its formation; see Figure 4. To conclude, under the conditions studied, the theoretical models C3 and C4 are in excellent agreement with the experimental findings, both in terms of the calculated hydrogen-induced binding energy shifts of the respective undercoordinated atoms and in terms of the hydrogen coverage.

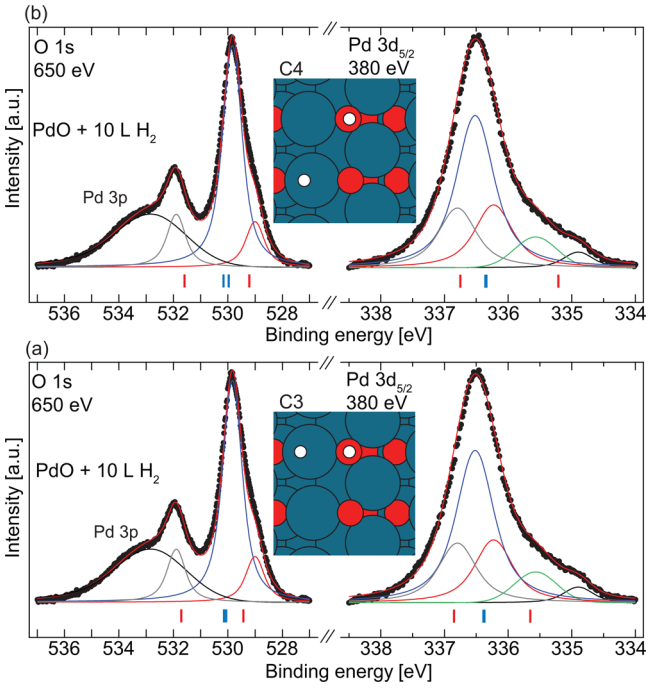

Figure 6. Hydrogen adsorption on the PdO(101) surface. HRCL spectra from the O 1s (left) and Pd $3d_{5/2}$ (right) regions together with the calculated binding energy shifts for the most probable configurations C3 and C4 (see text). The calculated CLS are indicated by the red (3-fold) and blue (4-fold) lines underneath each spectrum. The shift toward lower binding energy of the Pd_{3f} is not resolved experimentally. It shall be noted that the calculated CLS for the Pd_{4f} is lower with respect to the experimental value, and therefore, the calculated value for Pd_{3f}-H appears at slightly lower binging energy.

C. Desorption of Hydrogen. We have investigated the desorption of the adsorbed hydrogen species on the PdO(101) surface by flashing the surface after hydrogen adsorption at 110 K to different temperatures and recording the corresponding O 1s spectra after cooling to 110 K. The data are shown in Figure 7a. The areas under the O_{3f}-H, the O_{3f}, and the O_{4f} peaks are

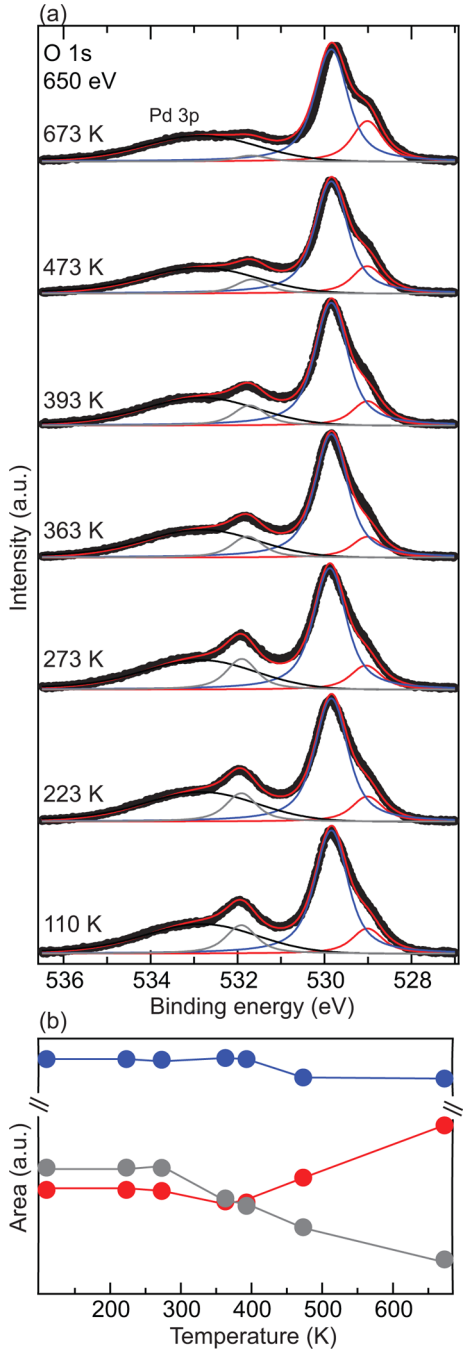

Figure 7. Heating sequence of the hydroxide covered surface: (a) O 1s spectra recorded with a photon energy of 650 eV. (b) Intensity of O 1s OH component (gray) and oxide components (red and blue) as a function of temperature.

dx.doi.org/10.1021/jp4036698 | J. Phys. Chem. C 2013, 117, 13510−13519

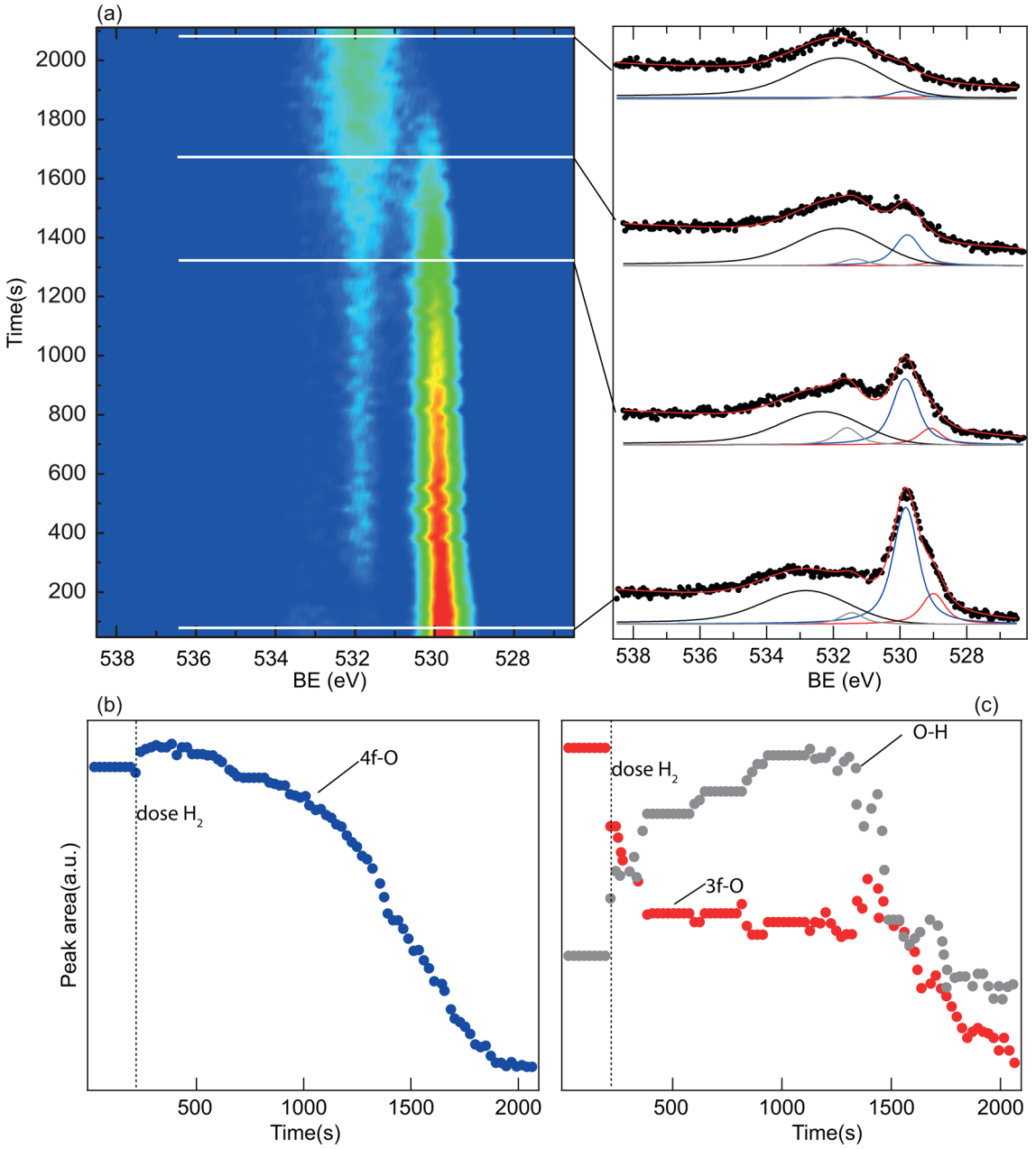

Figure 8. (a) Hydrogen-induced reduction using a H_2 partial pressure of 1×10^{-8} mbar and a sample temperature of 300 K of the PdO surface. The evolution of the O 1s level as a function of time is shown in the left panel, whereas some selected spectra during the reduction process are shown to the right. (b) The extracted area for the O_{4f} and (c) OH and O_{3f} components as a function of time during the reduction of the PdO(101) by hydrogen.

reported in Figure 7b. No differences between the spectra obtained at 110 K and the spectra obtained after flashing at 223 and 273 K could be observed, which implies that there are no structural changes between these temperatures. At a temperature of 363 K, a slight decrease in the O_{3f}-H component is observed. This trend of a decreasing amount of OH on the surface is even more pronounced at 393 K, and the component in the O_{3f} binding energy region is, surprisingly, increasing in intensity. Notably, the temperature range over which our measurements reveal a loss of OH groups from the surface agrees well with the temperature range spanned by the H_2O desorption feature observed in previous TPD experiments of H_2 oxidation on PdO(101).[27] At higher temperatures, the O_{3f}-H component has almost vanished, and the component in the O_{3f} binding energy region has regained the same intensity as that observed for the clean PdO(101) surface.

Why is the intensity in the binding energy region of the O_{3f} component increasing as the OH is disappearing from the surface? One interpretation would be that the H is desorbing from the surface, thereby restoring a clean PdO(101) surface. However, this interpretation is not likely because water is known to form when a hydrogen-exposed PdO(101) surface is heated.[27] A second interpretation is that, assuming that water is being produced and desorbing, the remaining surface will correspond to that in model C7 in Figure 5. The calculations show that, in this structure, the surface O_{4f} component will exhibit a negative CLS similar to that of the O_{3f} component. This could explain the increasing intensity in this binding

dx.doi.org/10.1021/jp4036698 | J. Phys. Chem. C 2013, 117, 13510−13519

energy region as the OH groups are being removed upon water formation and desorption. Thus, after the water desorption, the O_{3f} component obtains contributions from both the remaining O_{3f}-H groups (models C3 and C4) as well as areas on the surface that correspond to model C7. Furthermore, recent STM experiments[40] show that more substantial restructuring processes also restore O_{3f} atoms when the PdO(101) surface is thermally reduced at elevated temperature. Specifically, the STM results reveal that pristine PdO(101) surface layers are regenerated at 720 K during the thermal reduction of PdO(101) films by a mechanism wherein oxygen atoms from the subsurface of the PdO(101) film migrate to the surface and reoxidize reduced domains that are produced as the oxide decomposes. Similar restructuring processes may contribute to the replenishment of O_{3f} atoms observed in the present study, particularly at the higher temperatures investigated.

It is also clear from the data shown in Figure 7 that water is not present on the surface while heating, as, in that case, a component shifted by 3.4 eV with respect to the O_{4f} component should have been observed (model C6 in Figure 5). However, as it is known that water may form and desorb from the PdO(101) surface,[27] it is likely that water is formed also in the present experiments but that it desorbs instantly and cannot be detected by HRCLS. The reaction pathway predicted by the present calculations (Figure 4) is consistent with this interpretation. In particular, the calculations predict that the most energetically demanding step in the water formation process is the hopping of a H atom from a Pd_{3f} atom to an O_{3f} atom (C4 to C5 in Figure 4). The high barrier for H-hopping, suggests that the rate of H-hopping to an O_{3f} atom could determine the net rate of H_2O desorption; that is, water desorption is a reaction-limited process in this system. Interestingly, as the predicted barriers for H-hopping and water desorption are comparable, it is reasonable to expect that the desorption of water in this case would occur over a similar range of temperature as the desorption-limited evolution of adsorbed water molecules from PdO(101). Consistent with this interpretation, prior studies reveal that the H_2O TPD feature resulting from H_2 oxidation on PdO(101)[27] overlaps closely with the H_2O TPD peak obtained from water-covered PdO(101),[45] with both features appearing mainly between 300 and 400 K. We note that, because the barriers for H-Pd to H-O hopping and water desorption are very similar, the hopping step cannot be definitively assigned as the rate-controlling step without additional information. At the least, the results suggest that the hopping step occurs at a similar rate as water desorption, and thus limits water accumulation on the surface.

D. Hydrogen-Induced Reduction of PdO(101) at Room Temperature. The hydrogen interaction with a PdO(101) surface was also studied at room temperature. The data are presented in Figure 8a. The O 1s level from a PdO(101)-covered Pd(111) surface was recorded as a function of time at a surface temperature of 300 K and a constant hydrogen (H_2) background of 1×10^{-8} mbar. In Figure 8b, we show the change of the area under the O_{4f} component. It can be observed that the reduction of the PdO is initially slow up to about a 1000 s of exposure but accelerates at higher exposure times. In Figure 8c, we show the change of the area under the O_{3f} and the O_{3f}-H components. The formation of OH groups is observed as soon as hydrogen is exposed to the surface, as evidenced by the appearance of the O_{3f}-H component and the concurrent decrease of the O_{3f} intensity. The O_{3f}-H component is increasing in intensity until approximately 1000 s while the O_{3f} component is more or less constant, consistent with the combined removal of O_{3f} atoms due to water desorption and the appearance of areas corresponding to that in model C7 in Figure 5. At exposure times higher than 1000 s, both the O_{3f} and the O_{3f}-H components are rapidly decreasing in intensity.

Again, no water component could be observed in the O 1s spectra at any time during these experiments. We thus conclude that water does not accumulate on the surface at room temperature, but rather desorbs immediately upon forming, as explained in the previous section.

The reduction process may be described as follows: initially, hydrogen adsorbs dissociatively on the Pd_{3f} atoms, forming Pd_{3f}-H and O_{3f}-H. At a high enough temperature, the OH may react with another H atom, forming H_2O that immediately desorbs from the surface, thereby reducing the oxide. This creates a surface structure according to model C7 in Figure 4 and more sites for dissociation and, thus, water formation. As the oxide is reduced, larger areas of model C7 are created and the reaction rate increases. A similar autocatalytic behavior has been observed for the thermal reduction of PdO(101) films[40] and a thin trilayer Rh oxide on Rh.[46]

V. SUMMARY

We have presented an experimental and computational study of the adsorption of hydrogen on PdO(101). The HRCLS measurements provide resolution to distinguish between Pd atoms at the PdO(101) surface coordinated to three or four oxygen atoms, thus providing a fingerprint for the under-coordinated Pd atoms. With the use of HRCLS, we observed that both the Pd and the O atoms are affected by the adsorption of hydrogen at 110 K. A core-level shift for the undercoordinated Pd atoms at the surface of the Pd oxide (Pd_{3f}) was observed together with a large shift of the surface O atoms. On the basis of DFT calculations, we have suggested that hydrogen adsorbs molecularly on the undercoordinated Pd atoms of the PdO(101) surface and dissociates to form Pd-H and O-H groups, with only half of the undercoordinated surface atoms being affected at 110 K. The proposed models are supported by the calculated Pd 3d and O 1s CLS, which agree well with the experimentally observed shifts. As the experimental HRCLS data provides no evidence of adsorbed water, we conclude that water formation does not occur upon hydrogen adsorption on PdO(101) at low temperatures. It was found, however, that hydrogen completely reduces the oxide at room temperature. Consistent with these observations, our DFT calculations predict that H_2 dissociation is facile on PdO(101) but that subsequent reaction steps that lead to water formation are more strongly activated, with energy barriers that are comparable to that for water desorption. The adsorption measurements support the assignment of the undercoordinated Pd and O atoms at the surface of the PdO(101) film. Moreover, the information reported in this study may be useful for understanding the dehydrogenation of hydrocarbons and other organic molecules over Pd.

■ AUTHOR INFORMATION

Corresponding Author

*Tel: +46 46 222 41 54. E-mail address: Edvin.Lundgren@sljus.lu.se.

Notes

The authors declare no competing financial interest.

■ ACKNOWLEDGMENTS

The Max IV staff is gratefully acknowledged. This work was financially supported by the foundation for strategic research (SSF), the Swedish Research Council, the Crafoord Foundation, the Knut and Alice Wallenberg Foundation, the Anna and Edwin Berger Foundation, and NordForsk. The Competence Centre for Catalysis (KCK) is hosted by Chalmers University of Technology and financially supported by the Swedish Energy Agency and the member companies: AB Volvo, ECAPS AB, Haldor Topsøe A/S, Scania CV AB, and Volvo Car Corporation AB. The calculations were performed at C3SE (Göteborg and PDC (Stockholm) via an SNIC grant. We also acknowledge the Ohio Supercomputing Center for providing computational resources. Lastly, J.F.W. and A.A. gratefully acknowledge financial support for this work provided by the U.S. Department of Energy, Office of Basic Energy Sciences, Catalysis Science Division, through Grant DE-FG02-03ER15478.

■ REFERENCES

(1) Hendriksen, B. L. M.; Bobaru, S. C.; Frenke, J. W. M. Oscillatory CO Oxidation on Pd(100) Studied With in Situ Scanning Tunneling Microscopy. *Surf. Sci.* **2004**, *552*, 229−242.

(2) Gao, F.; Wang, Y.; Cai, Y.; Goodman, D. W. CO Oxidation on Pt-Group Metals From Ultrahigh Vacuum to Near Atmospheric Pressures. 2. Palladium and Platinum. *J. Phys. Chem. C* **2009**, *113*, 174−181.

(3) Van Rijn, R.; Balmes, O.; Resta, A.; Wermeille, D.; Westerström, R.; Gustafson, J.; Felici, R.; Lundgren, E.; Frenken, J. W. M. Surface Structure and Reactivity of Pd(100) During CO Oxidation Near Ambient Pressures. *Phys. Chem. Chem. Phys.* **2011**, *13*, 13167−13171.

(4) Blomberg, S.; et al. In Situ X-ray Photoelectron Spectroscopy of Model Catalysts: At the Edge of the Gap. *Phys. Rev. Lett.* **2013**, *110*, 117601−117605.

(5) Burch, R.; Urbano, F. J. Investigation of the Active State of Supported Palladium Catalysts in the Combustion of Methane. *Appl. Catal., A* **1995**, *124*, 121−138.

(6) Burch, R.; Urbano, F. J.; Loader, P. K. Methane Combustion Over Palladium Catalysts: The Effect of Carbon Dioxide and Water on Activity. *Appl. Catal., A* **1995**, *123*, 173−184.

(7) Salmonsson, P.; Johansson, S.; Kasemo, B. Methane Oxidation Over PdO_x: On the Mechanism for the Hysteresis in Activity and Oxygen Content. *Catal. Lett.* **1995**, *33*, 1−13.

(8) Hellman, A.; et al. The Active Phase of Pd During Methane Oxidation. *J. Phys. Chem. Lett.* **2012**, *3*, 678−682.

(9) Weaver, J. F. Surface Chemistry of Late Transition Metal Oxides. *Chem. Rev.* **2013**, *113*, 4164−4215.

(10) Over, H. Surface Chemistry of Ruthenium Dioxide in Heterogeneous Catalysis and Electrocatalysis: From Fundamental to Applied Research. *Chem. Rev.* **2012**, *112*, 3356−3426.

(11) Over, H. Ruthenium Dioxide, a Fascinating Material for Atomic Scale Surface Chemistry. *Appl. Phys. A: Mater. Sci. Process.* **2002**, *75*, 37−44.

(12) Over, H.; Kim, Y. D.; Seitsonen, A. P.; Wendt, S.; Lundgren, E.; Schmid, M.; Varga, P.; Morgante, A.; Ertl, G. Atomic-Scale Structure and Catalytic Reactivity of the RuO_2(110) Surface. *Science* **2002**, *287*, 1474−1476.

(13) Over, H.; Seitsonen, A. P.; Lundgren, E.; Schmid, M.; Varga, P. Direct Imaging of Catalytically Important Processes in the Oxidation of CO over RuO_2(110). *J. Am. Chem. Soc.* **2001**, *123*, 11807−11808.

(14) Knapp, M.; Crihan, D.; Seitsonen, A. P.; Lundgren, E.; Resta, A.; Andersen, J. N.; Over, H. Complex Interaction of Hydrogen with the RuO_2(110) Surface. *J. Phys. Chem. C* **2007**, *111*, 5363−5373.

(15) Klikovits, J.; Napetschnig, E.; Schmid, M.; Seriani, N.; Dubay, O.; Kresse, G.; Varga, P. Surface Oxides on Pd(111): STM and Density Functional Calculations. *Phys. Rev. B* **2007**, *76*, 045405.

(16) Westerström, R.; et al. Stressing Pd Atoms: Initial Oxidation of the Pd(110) Surface. *Surf. Sci.* **2008**, *602*, 2440−2447.

(17) Westerström, R.; et al. Lack of Surface Oxide Layers and Facile Bulk Oxide Formation on Pd(110). *Phys. Rev. B* **2009**, *80*, 125431.

(18) Todorova, M.; et al. The Pd(100)−($\sqrt{5} \times \sqrt{5}$) R27°-O Surface Oxide Revisited. *Surf. Sci.* **2003**, *541*, 101−112.

(19) Zheng, G.; Altman, E. I. The Oxidation of Pd(111). *Surf. Sci.* **2000**, *462*, 151−168.

(20) Lundgren, E.; Kresse, G.; Klein, C.; Borg, M.; Andersen, J. N.; De Santis, M.; Gauthier, Y.; Konvicka, C.; Schmid, M.; Varga, P. Two-Dimensional Oxide on Pd(111). *Phys. Rev. Lett.* **2002**, *88*, 246103.

(21) Kan, H. H.; Weaver, J. F. A PdO(1 0 1) Thin Film Grown on Pd(1 1 1) in Ultrahigh Vacuum. *Surf. Sci.* **2008**, *602*, L53−L57.

(22) Kan, H. H.; Weaver, J. F. Mechanism of PdO Thin Film Formation During the Oxidation of Pd(1 1 1). *Surf. Sci.* **2008**, *603*, 2671−2682.

(23) Gabash, H.; Unterberger, W.; Hayek, K.; Klötzer, B.; Kresse, G.; Klein, C.; Schmid, M.; Varga, P. Growth and Decay of the Pd(111)−Pd_5O_4 Surface Oxide: Pressure-Dependent Kinetics and Structural Aspects. *Surf. Sci.* **2006**, *600*, 205−218.

(24) Westerström, R.; et al. Oxidation and Reduction of Pd(100) and Aerosol-Deposited Pd Nanoparticles. *Phys. Rev. B* **2011**, *83*, 115440.

(25) Blanco-Rey, M.; Wales, D. J.; Jenkins, S. J. Mechanisms for H_2 Reduction on the PdO{101} Surface and the Pd{100}-($\sqrt{5} \times \sqrt{5}$) *R*27°-O Surface Oxide. *J. Phys. Chem. C* **2009**, *113*, 16757−16765.

(26) Cox, J. D.; Wagman, D. D.; Medvedev, V. A. *CODATA Key Values for Thermodynamics*; Hemisphere Publishing Corp.: New York, 1989.

(27) Hakanoglu, C.; Hawkins, J. M.; Asthagari, A.; Weaver, J. F. Strong Kinetic Isotope Effect in the Dissociative Chemisorption of H_2 on a PdO(101) Thin Film. *J. Phys. Chem. C* **2010**, *114*, 11485−11497.

(28) Nyholm, R.; Anderssen, J. N.; Johansson, U.; Jensen, B.; Lindau, I. Beamline I311 at MAX-LAB: A VUV/Soft X-ray Undulator Beamline for High Resolution Electron Spectrocopy. *Nucl. Instrum. Methods Phys. Res., Sect. A* **2001**, *467−468*, 520−524.

(29) Perdew, J. P.; Burke, K.; Ernzerhof, M. Generalized Gradient Approximation Made Simple. *Phys. Rev. Lett.* **1996**, *77*, 3865−3868.

(30) Kresse, G.; Hafner, J. Ab Initio Molecular-Dynamics Simulation of the Liquid-Metal-Amorphous−Semiconductor Transition in Germanium. *Phys. Rev. B* **1994**, *49*, 14251−14269.

(31) Kresse, G.; Furthmüller, J. Efficiency of ab-Initio Total Energy Calculations for Metals and Semiconductors Using a Plane-Wave Basis Set. *Comput. Mater. Sci.* **1996**, *6*, 15−50.

(32) Kresse, G.; Furthmüller, J. Efficient Iterative Schemes for ab Initio Total-Energy Calculations Using a Plane-Wave Basis Set. *Phys. Rev. B* **1996**, *54*, 11 169−11 186.

(33) Blöchl, P. E. Projector Augmented-Wave Method. *Phys. Rev. B* **1994**, *50*, 17953−17979.

(34) Kresse, G.; Joubert, D. From Ultrasoft Pseudopotentials to the Projector Augmented-Wave Method. *Phys. Rev. B* **1999**, *59*, 1758−1775.

(35) Monkhorst, H. J.; Pack, J. D. Special Points for Brillouin-Zone Integrations. *Phys. Rev. B* **1976**, *13*, 5188−5192.

(36) Pack, J. D.; Monkhorst, H. J. "Special points for Brillouin-zone integrations"—A Reply. *Phys. Rev. B* **1977**, *16*, 1748−1749.

(37) Henkelman, G.; Uberuaga, B. P.; Jónsson, H. A Climbing Image Nudged Elastic Band Method for Finding Saddle Points and Minimum Energy Paths. *J. Chem. Phys.* **2000**, *113*, 9901−9904.

(38) Pehlke, E.; Scheffler, M. Evidence for Site-Sensitive Screening of Core Holes at the Si and Ge(001) Surface. *Phys. Rev. Lett.* **1993**, *71*, 2338−2341.

(39) Nilsson, P. O.; Shivaraman, M. S. Optical Properties of PdO in the Range of 0.5-5.4 eV. *J. Phys. C: Solid State Phys.* **1979**, *12*, 1423−1427.

(40) Hinojosa, J. A., Jr.; Weaver, J. F. Surface Structural Evolution During the Thermal Decomposition of a PdO(101) Thin Film. *Surf. Sci.* **2011**, *605*, 1797−1806.

(41) Rogal, J.; Reuter, K.; Scheffler, M. Thermodynamic Stability of PdO Surfaces. *Phys. Rev. B* **2004**, *69*, 075421.

(42) Seriani, N.; Harl, J.; Mittendorfer, F.; Kresse, G. A First-Principles Study of Bulk Oxide Formation on Pd(100). *J. Chem. Phys.* **2009**, *131*, 054701.
(43) Kasper, N.; Nolte, P.; Stierle, A. Stability of Surface and Bulk Oxides on Pd(111) Revisited by In-Situ X-ray Diffraction. *J. Phys. Chem. C* **2012**, *116*, 21459−21464.
(44) Paz-Borbon, L. O.; Hellman, A.; Grönbeck, H. Simulated Photoemission Spectra of Hydroxylated MgO(100) at Elevated Temperatures. *J. Phys. Chem. C* **2012**, *116*, 3545−3551.
(45) Kan, H. H.; Colmyer, R. J.; Asthagiri, A.; Weaver, J. F. Adsorption of Water on a PdO(101) Thin Film: Evidence of an Adsorbed HO−H_2O Complex. *J. Phys. Chem. C* **2009**, *113*, 1495−1506.
(46) Klikovits, J.; Schmid, M.; Gustafson, J.; Mikkelsen, A.; Resta, A.; Lundgren, E.; Andersen, J. N.; Varga, P. Kinetics of the Reduction of the Rh(111) Surface Oxide: Linking Spectroscopy and Atomic-Scale Information. *J. Phys. Chem. B* **2006**, *110*, 9966−9975.